

Article

Digital Pole Control for Speed and Torque Variation in an Axial Flux Motor with Permanent Magnets

Adrián González-Parada ^{1,*}, José Merced Lozano-García ¹ and Mario Alberto Ibarra-Manzano ²¹ Electrical Department, DICIS University of Guanajuato, Salamanca 36885, Mexico; jm.lozano@ugto.mx² Electronics Department, DICIS University of Guanajuato, Salamanca 36885, Mexico; ibarram@ugto.mx

* Correspondence: gonzaleza@ugto.mx

Abstract: The use of renewable energies in the transportation industry has prompted the development of higher power electric motors and intelligent electronic traction systems. However, the typical coupling between the two continues to be mechanical, which reduces its efficiency and useful life. On the other hand, permanent magnet axial flux motor configurations make it possible to dispense with mechanical couplings, due to their high torque at low speeds due to their direct application on the wheels of vehicles. In this work, the design of a digital pole commutation system is presented, applied to an axial flux motor with permanent magnets for speed and torque control at a constant speed. The performance of the system is evaluated with experimental measurements; proving the effectiveness of the design, obtaining torques of up to 1784 Nm without extra mechanical couplings and maximum speed regulation errors of 8.43%.

Keywords: digital control; pole commutation; axial flux motor



Citation: González-Parada, A.; Lozano-García, J.M.; Ibarra-Manzano, M.A. Digital Pole Control for Speed and Torque Variation in an Axial Flux Motor with Permanent Magnets. *Electronics* **2022**, *11*, 482. <https://doi.org/10.3390/electronics11030482>

Academic Editor: Jose Eugenio Naranjo

Received: 12 October 2021

Accepted: 28 January 2022

Published: 7 February 2022

Publisher's Note: MDPI stays neutral with regard to jurisdictional claims in published maps and institutional affiliations.



Copyright: © 2022 by the authors. Licensee MDPI, Basel, Switzerland. This article is an open access article distributed under the terms and conditions of the Creative Commons Attribution (CC BY) license (<https://creativecommons.org/licenses/by/4.0/>).

1. Introduction

The entry of electric motors (EM) in the automotive industry in conjunction with the advancement and accessibility to the power electronics controlled by digital systems has led to the development of motors with emerging technologies such as permanent magnet motors (PMM), commutable reluctance motors (CRM) and reluctance synchronous motors that exceed 95% efficiency. Despite the great development in areas of design and operation of EM; These, like internal combustion engines, continue to depend on mechanical systems such as gear trains (transmission systems) to convert their high speed with low torque to low speeds with high torque, resulting in more expensive, heavy, inefficient applications and more susceptible to failures than they should be [1].

EMs are currently being used as an essential part of the development of hybrid vehicles (HV) and electric vehicles (EV); thus, avoiding generating less or no hydrocarbon consumption [2,3]. The HV and EV use a synchronous radial flow electric motor/generator (RFM), which partially or totally develops the required torque for the movement of the vehicle, such applications have led to the use and investigation of unconventional configurations of electric motors, such as axial flow motors (AFM), in HV and EV applications due to their multiple advantages [4]. Some advantages of AFM over RFM have been demonstrated, such as a higher ratio of active volume–power, greater torque, and efficiency [5–7].

In a different way, speed control in alternating current electric motors can be developed through mechanical and electrical means. The first of these means is the use of gear trains, which through gears with different numbers of teeth, form the speed transformation ratio. However, these mechanical systems do not modify the engine speed as such, but a relative speed is acquired which is always less than or equal to the original speed delivered, this characteristic makes these systems limited, expensive and bulky. However, the electric speed control means depend on the power supply frequency and the number of poles of the motor.

The electrical power frequency as a method to modify the speed of an AC motor has been extensively studied, due to design tools based on pulse width modulation (PWM) techniques, such technology turns out to be cheap as well as accurate [8]. Despite, the disadvantages that the PWM based control has been evident at low speeds; in which it loses precision in the applied torque at low speeds, making it necessary to add an additional control [9]. As low speed control applications are common today, due to the rise of HV and EV, the alternative to improve the performance of an RFM at low speeds without using extra mechanisms, is the use of EM in which its functional configuration allows the increase of poles and/or phases of the motor. An example of these motors is the commutable reluctance motor, where the improvement in the performance of speed and torque by increasing the number of poles, causing a greater balance of magnetomotive forces (MMF) [10]. However, when increasing the number of poles in an RFM, there is also an increase in iron losses, switching losses and inconveniences in the installation of position sensors due to this [11,12].

In addition to this, in recent studies as in the case of Magill [13] have been modeled and designed RFM, using speed control methods based on amplitude modulation phase, such methods have also been tried in applications for EV [14]. This technique involves switching and selecting the number of poles indirectly. While in other research it takes advantage of the new semiconductor technology based on silicon carbide (SiC), to raise a technique speed change in RFM, directly modifying the configuration of the windings and poles in the stator, achieving a broad range for EV applications [15].

Speed–torque control and change operations such as, i.e., velocity, are other means through which it is possible to impact EM performance. One of the most exploited methods in MFR configurations is PWM, however, previous works have shown the most significant disadvantage of this method, which is the generation of disturbances in the operation of the RFM, seeing the need to add an additional control to avoid such disturbance [16]. Furthermore, other RFM configurations such as commutable reluctance motors (RCM), allow a control method based on the electronic commutation of their windings, using isolated gate bipolar transistors (IGBT) as switching circuits, in addition to requiring a digital system for its operation. Such a method does not have the disadvantage of generating disturbances in the electromagnetic performance of the motor, in addition to being simpler. Due to the design of the RFM, it is possible to migrate the aforementioned techniques for speed and torque control in RFM to AFM. The use of the PWM technique for the control of axial flow motors has been explored [17].

The contributions of the previous works have shown the drawbacks of PWM control techniques, such as adding additional controls, while in the case of pole commutation there are problems in the installation of the necessary position sensors and an increase in motor losses. Consequently, the next step in the research and use of EM in HV and EV applications is the design of simpler digital speed control systems, dispensing with and/or reducing the number of necessary sensors, with the ability to deliver high and stable torque without using extra mechanisms.

2. Methods

2.1. Control Theory

Rotation in permanent magnet motors (PMM) is produced by the interaction of an alternating magnetic field in the presence of a static magnetic field. This interaction generates attraction-repulsion forces depending on the magnetic polarity present. The most common configurations of PMM are the radial type with brushes where the rotating part (rotor) is inside the static part (stator), the alternating magnetic field is produced by means of a mechanical switching system, called a slip ring.

The number of magnetic poles in the stator (SMP) and magnetic poles in the rotor (RMP) are other characteristics of PMMs that it includes in its performance and control. To demonstrate it, a motor with the configuration of two RMP and three SMP is shown in Figure 1. The SPM are identified as: C1, C2 and C3; while the north magnetic pole (NP) and

south magnetic pole (SP) in the rotor are identified with the plus sign (+) and the minus sign (-), respectively.

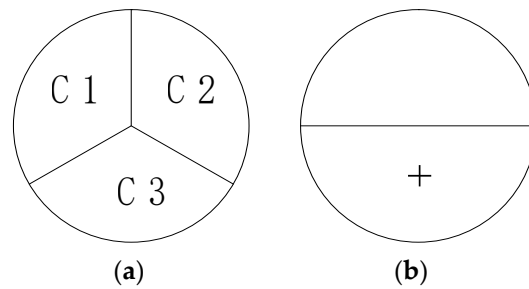


Figure 1. Electric motor with 3 magnetic poles in stator, and 2 magnetic poles in rotor: (a) 3 magnetic poles stator; (b) 2 magnetic pole rotors.

To develop a clockwise rotational movement in the configuration of Figure 1, SPM C1, C2 and C3 must be set as SP, SP and NP, respectively; such a magnetic arrangement in SPMs is shown in the sequence 1 stator in Figure 2.

The magnetic configuration of the SPM of sequence 1 shown in Figure 2 will produce an attractive force on NP and SP of the rotor, forcing it to rotate 60 degrees to align with the magnetic field of the SPM. The rotor in sequence 2 of Figure 2 shows the resulting position caused by the application of magnetic distribution in the stator of sequence 1.

Thus, as the magnetic distribution of the stator is changed in the order shown (1, 2, 3, 4, 5, 6) in Figure 2, a force of attraction and repulsion will be applied to the rotor in each sequence, forcing it to take the position of the consecutive sequence, until it returns to the initial position (configuration 1). Therefore, to produce a complete revolution in the rotor of the configuration of Figure 2 is necessary to develop the six different magnetic configurations shown in Figure 2.

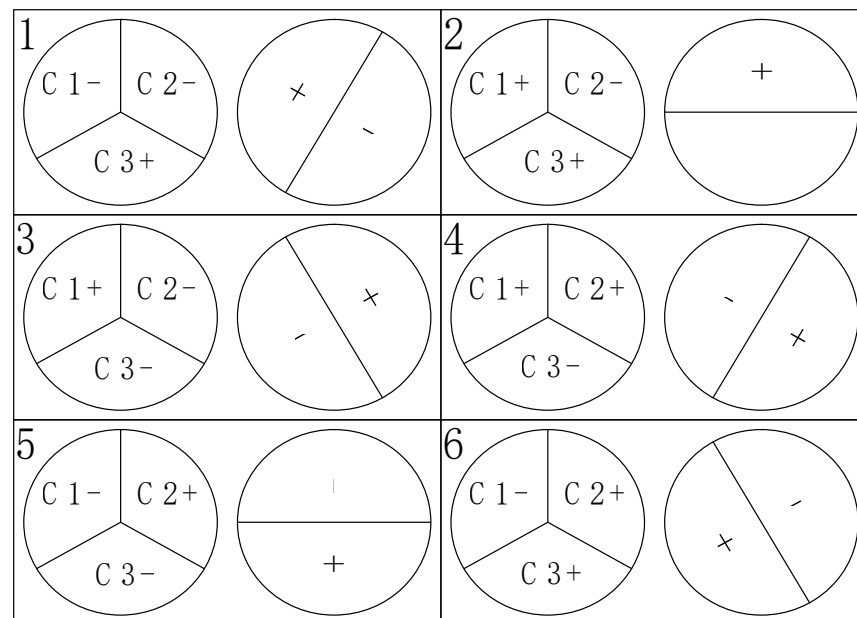


Figure 2. Magnetic sequences for rotation clockwise of the motor.

The magnetic polarity of the C1, C2 and C3 coils along twelve continuous sequences is shown in Figure 3, where it is seen that the three curves produce two full periods and are identical with a phase shift of $\pm 1/3$ cycle between them, this phase shift is the same as in the case of a three-phase sinusoidal signal.

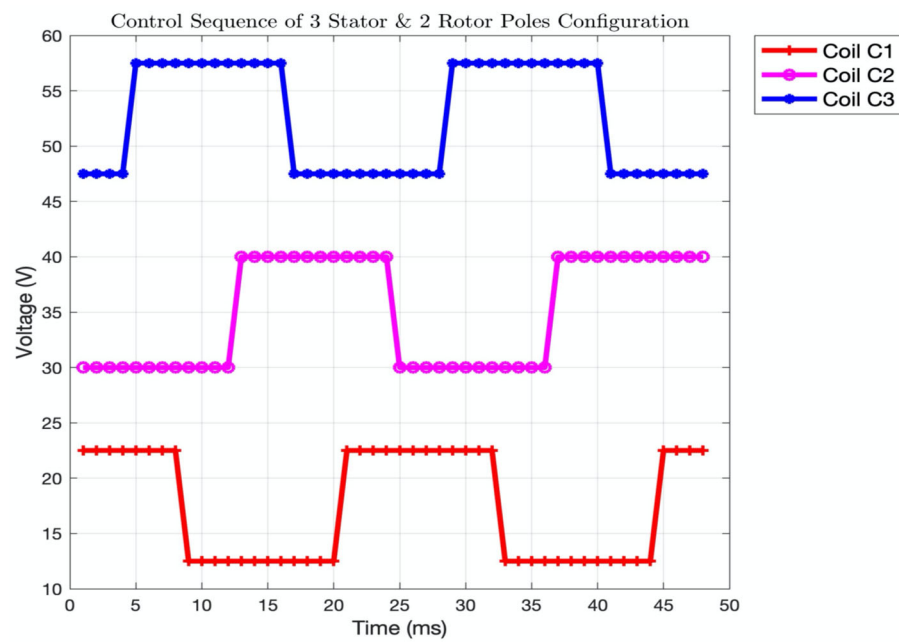


Figure 3. Magnetic polarization sequences in the three stator coils.

The above analysis is based on the number of SMP, and RMP can be extended for PMM with a different number of poles. Some results of this analysis are shown in Table 1. Where it is noted that the configurations with the number of SMP multiple of three ($3n$) and RMP number powers of two (2^n) produce an increase of twice the number of sequences per revolution (SPR) and electrical cycles per revolution ($ECPR$), without modifying the number of electrical phases to be used.

Table 1. Pole number analysis in a PMM.

Stator Pole	Rotor Pole	SPR	ECPR	Phase
3	2	6	1	3
3	4	12	2	3
6	2	6	3	2
6	4	12	2	3
9	8	24	4	3
12	16	48	8	3
15	32	96	16	3

It can be generalized in Table 2, where n is the order of the configuration for a motor with $3n$ SPM and 2^n RMP.

Table 2. Analysis of $3n$ poles in the stator and 2^n .

Order n	Stator Pole $SP = 3n$	Rotor Pole $RP = 2^n$	Seq./Rev. $SPR = (3) 2^n$	Electrical Cycles/Rev. $ECPR = 2^{n-1}$	Phase φ
1	3	2	6	1	3
2	6	4	12	2	3
3	9	8	24	4	3
4	12	16	48	8	3

2.2. Speed Control for $3n$ Stator and 2^n Rotor Configuration

For this study case, it is considered that the time required to change the PMEs from one SMP to another is depreciable and that the time that the PMEs remain active in each SMP is T_S seconds per sequence. Starting from the existing relationships shown in Table 2

for the PPM configuration with $3n$ SMP and 2^n RMP, it is obtained that, the rotational speed (S) in rpm for a PPM of order n is given by Equation (1)

$$S_{rpm} = \frac{1}{SPR} \frac{1}{T_s} \frac{60 \text{ seg}}{\text{min}} = \frac{5}{(2^{n-2})T_s} = \frac{5f_s}{2^{n-2}} \tag{1}$$

where:

- S_{rpm} —Rotational speed in rpm
- f_s —Sequencing frequency in sequences/second
- SPR —Sequences per revolution
- T_s —Activation time in sequences/second

The rotational speed, Equation (1), is dependent on sequencing time or frequency; However, through the dependence between the number of sequences per revolution (SPR) and the electrical cycles per revolution ($ECPR$), it is possible to establish a relationship between the sequential frequency and the electrical frequency as shown in Equation (2)

$$f_E = \frac{ECPR}{SPR} f_s = \frac{2^{n-1}}{(3)(2^n)} f_s = \frac{f_s}{6} = \frac{1}{6T_s} \tag{2}$$

where:

- f_E —Electric frequency in Hz
- $ECPR$ —Electric cycles per revolution
- SPR —Sequences per revolution
- f_s —Sequencing frequencies

Combining Equation (1) with Equation (2), we will obtain Equation (3), which is the rotational speed in terms of the electrical power frequency

$$S_{rpm} = \frac{30f_E}{2^{n-2}} = \frac{30}{(2^{n-2})T_E} \tag{3}$$

where:

- T_E —Period in which a complete cycle of the alternating signal develops.

Equation (3) is applicable for the case of a sinusoidal three-phase supply; Figure 4 shows the variation of the speed with respect to the electrical frequency (f_E) for different values of n .

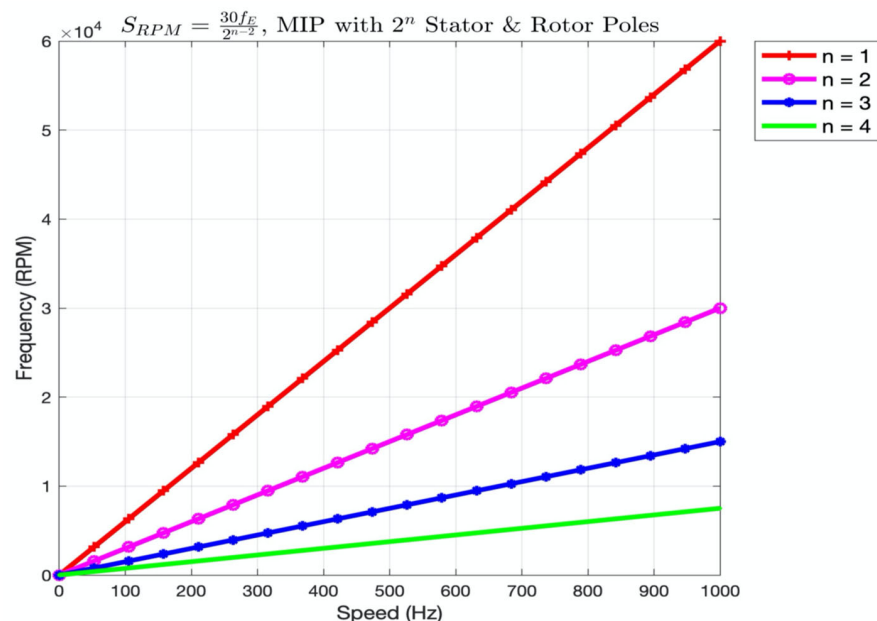


Figure 4. Speed with respect to electrical frequency.

The constitutive advantage of this type of speed control for the permanent magnet axial flux motor (AFMPM) with $3n$ poles in stator and 2^n poles in rotor is that when the order (n) increases, the type of power supply (three-phase), necessary for its operation, does not change.

Therefore, in this work, the use of a fourth-order configuration ($n = 4$) is proposed. That is, twelve ($3n = 12$) poles in the stator and sixteen ($2^n = 16$) poles in the rotor, because it is an economically feasible design with enough poles in the stator to evaluate different partial torque applications.

For the selected study case, the speed for AFMPM, according to Equation (3), is represented by Equation (4)

$$S_{rpm} = 7.5f_E = \frac{7.5}{T_E} \quad (4)$$

The AFMPM configuration allows modifying the applied torque, depending on the number of active poles in the stator coils. After having analyzed the possible coil (pole) switching modes per phase; For the previously selected study case of twelve ($3n = 12$) poles in the stator and sixteen ($2^n = 16$) poles in the rotor, six different operating torque settings (CT) of the AFM are proposed without affecting its speed where, torque setting 1 (CT1) produces the lowest possible mechanical power output, as the use of coils is restricted to a minimum (one coil per phase), while torque setting 6 (CT6) operates at maximum mechanical power possible output, due to the use of all the coils (four coils) per phase. In order to illustrate the process of switching for configuration, only the initial process (CT1) and the final one (CT6) are described, since the intermediate processes are handled between both ends.

In the operation mode for CT1, the stator magnetic field is developed using one coil per phase, each phase switches position in its four possible quadrants, for which it is necessary for four switching cycles for the phases to activate the induction coils again, to a quadrant again. The four quadrant switching cycles are shown in Figure 5.

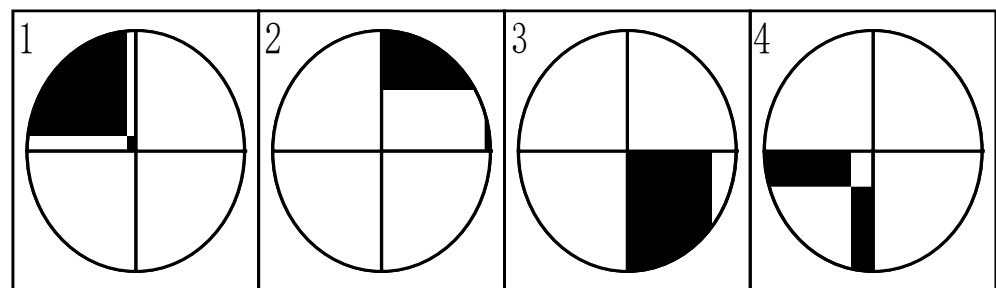


Figure 5. Switching sequences for CT1 configuration.

While in Figure 6 the respective commutation of the twelve coils in the stator for CT1 is shown, where the commutation signal for each coil has three different states, the positive activation state (portion of the rising curve), the state of negative activation (portion of the descending curve) and the state of non-activation (central portion of the curve).

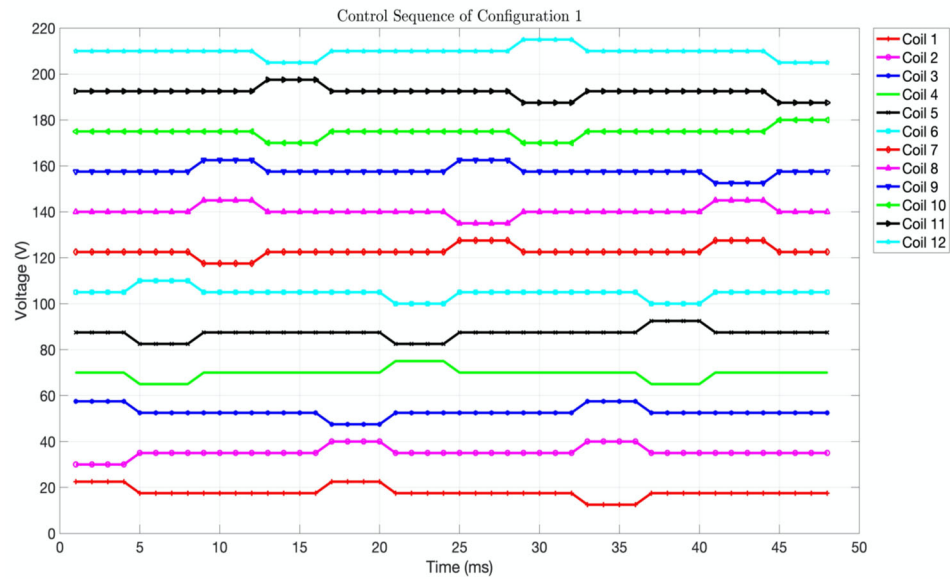


Figure 6. Switching signals of the twelve magnetic poles for CT1.

Alternatively, the proposed torque configuration 6 (CT6) makes use of all the coils in all the quadrants; for the CT6 any type of commutation (opposite or rotary) is negligible in its operation. Figure 7 shows the four switching cycles of the two quadrants for CT6.

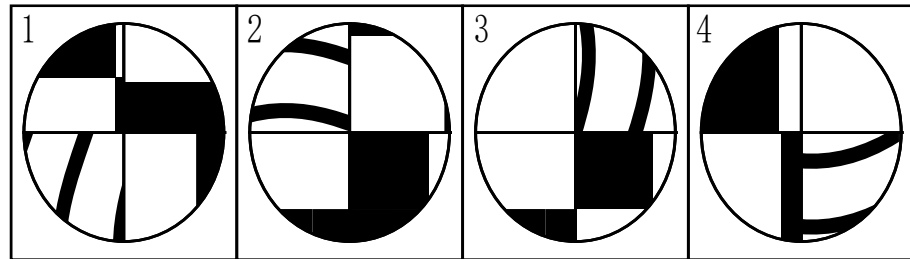


Figure 7. Switching sequences for CT6 configuration.

Figure 8 shows the switching sequence of the 12 coils in the stator for CT6.

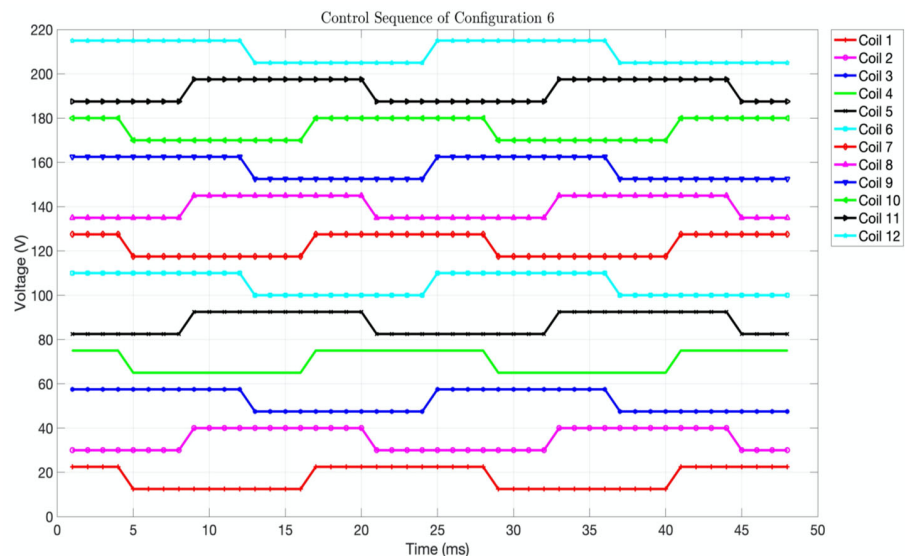


Figure 8. Switching signals of the twelve magnetic poles for CT6.

2.3. Speed and Torque Control Implementation

To combine a system that develops a three-phase frequency change, to modify the speed and also to allow the coils to be switched independently, in such a way as to modify the applied torque, a derived synchronization system with a clock generator is necessary; in this way, there will be a common clock that feeds a sequential machine (six sequences necessary for rotation) and generates additional clocks for the commutation of the coils. Considering the operations necessary for a digital system to perform speed control and torque control at constant speed, the block diagram of the system in Figure 9 is proposed.

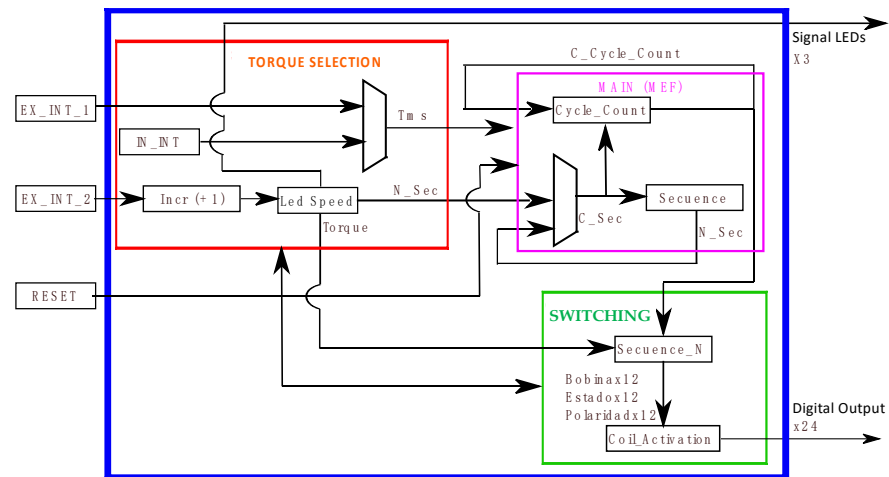


Figure 9. Block diagram of speed and torque control system.

This system is made up of three main blocks called TORQUE SELECTION, MAIN (MEF) and SWITCHING. Each block is dedicated to cover the required aspects *n* for the integration of the desired control. The red block called TORQUE SELECTION in Figure 9 carries out the selection of the desired torque configuration by the user through an external interrupt (EX_INT_2), it also establishes the period (Tms) that each of the six takes speed control sequences, through another external interrupt (EX_INT_1), this period could also be set or modified automatically with a programmed internal interrupt (IN_INT) to perform a smoother speed change.

The functional block in magenta color called MAIN (MEF) in Figure 9, establishes the achievement of the six sequences necessary to move the rotor $\pi/4$ radians in a cyclical manner, and the quadrant commutation previously exposed is developed. The Cycle Count function performs quadrant switching; For the case study, the quadrant commutation was performed every six operating sequences, in order to give more dead time to the non-active coils between commutations, which means more cooling time.

The green functional block called SWITCHING in Figure 9 has the functions responsible for activating and modifying the polarity of the coils (magnetic poles) in the stator based on the control signals received from the two previously mentioned functional blocks (TORQUE and MAIN SELECTION (MEF)). The output signals are twelve two-bit words, which will send the activation and polarity of the coil to the switching circuits; Table 3 shows the truth table for coil activation.

Table 3. Truth table and polarity for switching circuits.

b0	b1	Activation	Polarity
0	0	0	X
1	0	1	1
0	1	1	0
1	1	0	X

The values of one (1) and zero (0) in the activation column of Table 3 mean enabled and disabled, respectively; while for the column polarity 1, 0 and X mean positive polarity, negative polarity and it does not matter, respectively. Speed and torque sequence control applied can be implemented in digital systems, such as FPGAs and microcontrollers.

3. Results

For the speed and torque control system evaluation, it was applied to an axial flow motor with permanent magnets, where U-type coils were used in the stator according to the proposed configuration (12 coils). A configuration of neodymium permanent magnets of 16 pairs with different diameters was used in the rotor to cover the magnetic areas generated by the coils in the stator, in Figure 10 the construction of the motor used for the tests is shown.

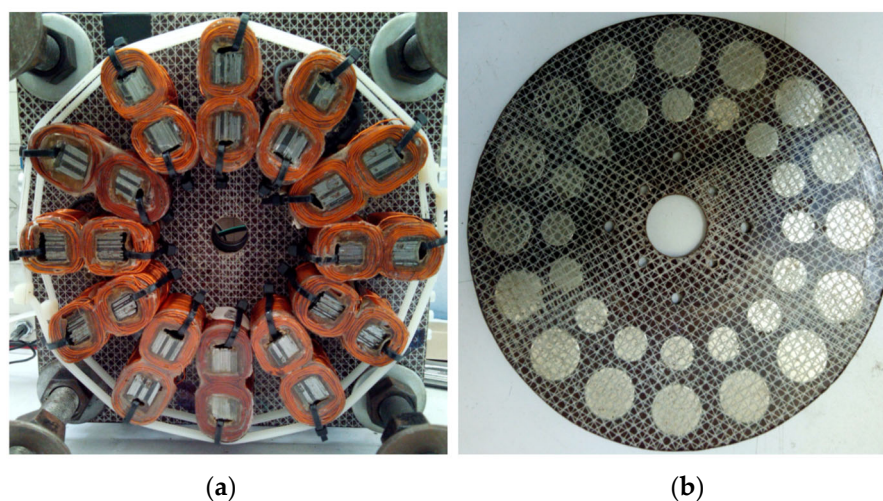


Figure 10. Permanent magnet axial flow motor prototype: (a) Motor stator; (b) Motor rotor.

The general dimensional characteristics of the permanent magnet motor in axial flow configuration are shown in Table 4.

Table 4. AFMPM general characteristics.

Parameter	Value	Unit
U-type core length	9.5	mm
Stator pole number	12	each
Rotor pole number	16	each
Minimum perimeter separation between larger and smaller magnets	4	mm
Number of core laminations	23	each
Lamination thickness	0.5	mm
Diameter of the largest magnet	19.0	mm
Diameter of the smaller magnet	12.7	mm

To measure the dynamic performance of the AFM, the Lab-Volt measurement system was implemented, which consists of the Lab-Volt 8960-A four-quadrant dynamometer/source module, configured in dynamometer mode to measure speed, torque and mechanical power delivered; the control–data acquisition interface, Lab-Volt Series 9063-02 and the open-source control and data acquisition software for electromechanical systems from Lab-Volt. Figure 11 shows the test system used for the AFM evaluation.

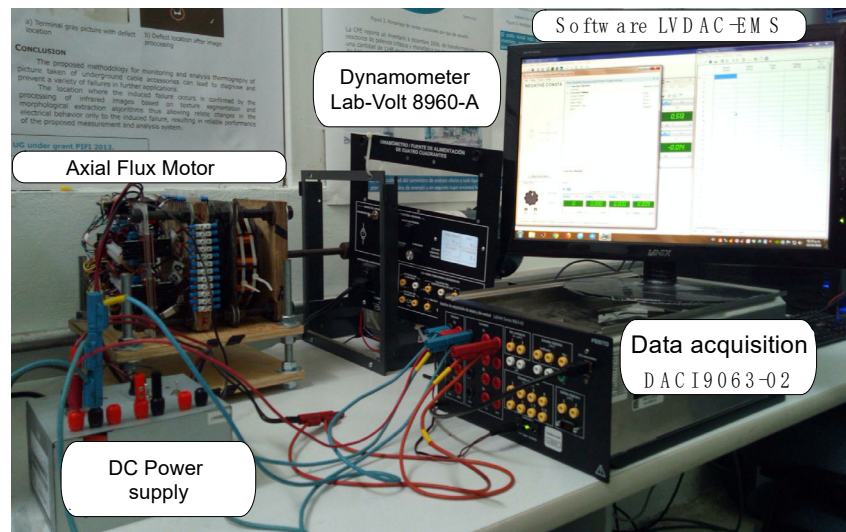


Figure 11. System used to measure dynamic characteristics.

The first measured dynamic characteristic was the change in angular velocity with respect to the change in the electrical supply frequency. The speed of the AFM was measured without load, while the electrical frequency was estimated by converting the digital switching frequency, developed by the speed control, into electrical frequency, using Equation (2). Figure 12 shows the graph of frequency–speed behavior, where on the horizontal axis there is the electrical power frequency and on the vertical axis the speed produced in the AFM.

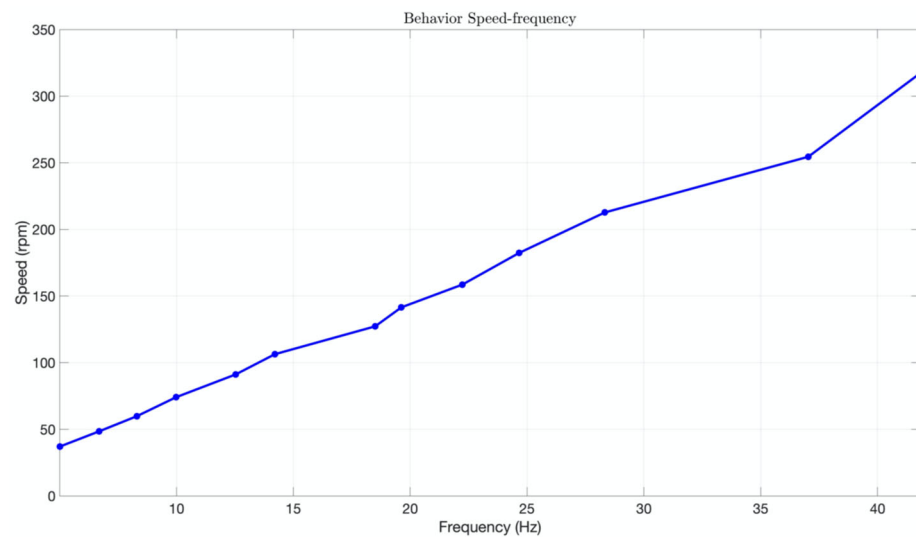


Figure 12. Behavior speed–frequency.

The next dynamic characteristic to measure was the torque provided by the AFM. Figure 13 shows the graphs of speed versus torque for each of the six proposed torque settings.

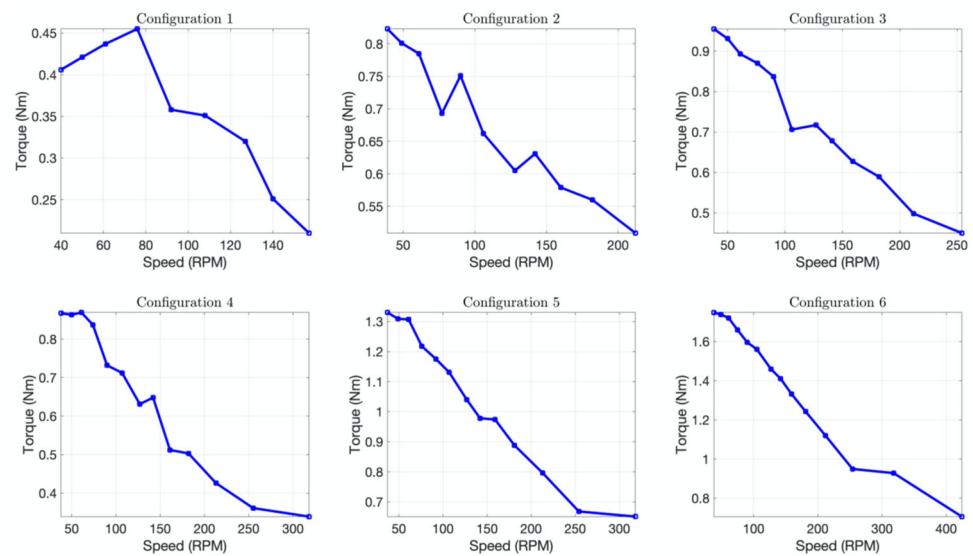


Figure 13. Speed–torque performance for all six configurations in AFM.

Based on the two previously measured dynamic characteristics (speed and torque) and according to Equation (5), it is possible to obtain the mechanical power delivered by the AFM in each of the six settings for controlling the speed and torque delivered

$$P = \frac{\tau S}{9,5493} \tag{5}$$

where:

- P —Generated power in watts
- τ —Generated torque in Nm
- S —Speed in rpm

According to Equation (5), the power speed graphs were obtained for each of the considered six configurations, these are shown in Figure 14.

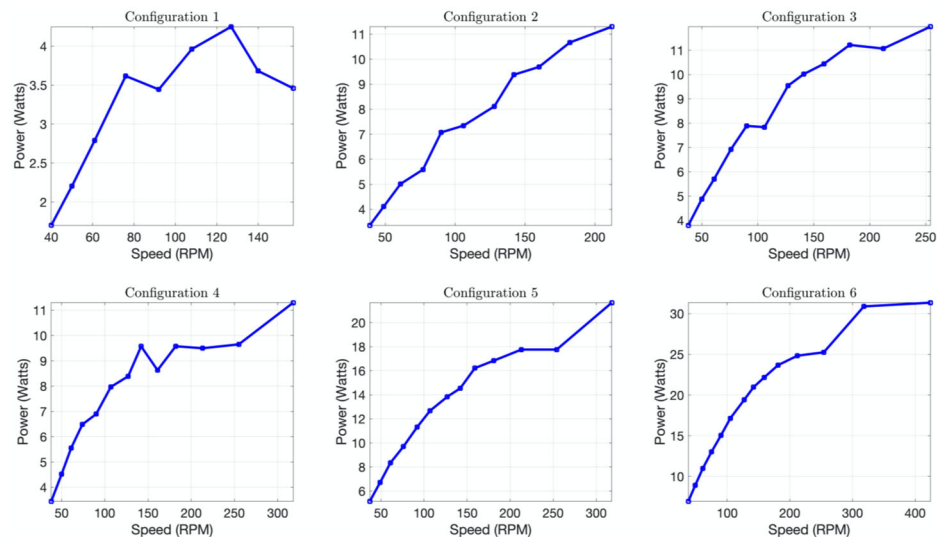


Figure 14. Speed–power performance for all six configurations in AFM.

As shown in Figures 13 and 14, the torque and maximum power developed for each configuration are different. Depending on the magnetic disturbances between the stator and the rotor, this is a point to improve that depends on the electrical design of the motor

and the optimization of the rotor to take full advantage of the magnetic field generated by the stator U coils.

The variations present in the curves of Figures 13 and 14 can be optimized by making the magnetic interaction between the permanent magnet rotor and the stator poles more efficient, these are due to the oscillation of the torque because at some point there are absences of the interaction of the magnetic field of the stator with respect to the rotor. Optimization must be focused on the rotor's magnetic field always interacting with the magnetic field produced by the stator, regardless of the configuration in which it is working.

4. Conclusions

In this work, the bases for digital control by electronic commutation of magnetic poles were established, in permanent magnet axial flow motors, with $3n/2^n$ poles in the stator/rotor.

The control was tested and evaluated on a modular AFMPM prototype; designed and built with electromagnetically isolated U-type coils, obtaining speeds of over 300 RPM, torques of up to 1784 Nm without extra mechanical couplings.

The most outstanding advantages of the developed control are the absence of sensors for speed control, the omission of extra mechanisms to produce high torque at low speeds, its simple implementation, and the possibility of being extended to conventional radial flow motor configurations.

The proposed control can limit the consumption of electrical energy without affecting the developed speed, making it ideal for applications in elevators, conveyors, regenerative braking systems and intelligent traction systems in electric and hybrid vehicles.

Author Contributions: Conceptualization, A.G.-P. and M.A.I.-M.; methodology, A.G.-P.; formal analysis, A.G.-P. and M.A.I.-M.; investigation, A.G.-P.; resources, J.M.L.-G.; data curation, A.G.-P. and J.M.L.-G.; writing—original draft preparation, A.G.-P.; writing—review and editing, J.M.L.-G. and M.A.I.-M.; project administration, A.G.-P.; funding acquisition, J.M.L.-G. and M.A.I.-M. All authors have read and agreed to the published version of the manuscript.

Funding: The APC was funded by the Universidad de Guanajuato.

Informed Consent Statement: Not applicable.

Acknowledgments: This project was fully supported by the Electronics and Electrical Departments of the Universidad de Guanajuato under the Program POA 2022.

Conflicts of Interest: The authors declare no conflict of interest.

References

1. Lambert, T.; Biglarbegian, M.; Mahmud, S. A Novel Approach to the Design of Axial-Flux Switched-Reluctance Motors. *Machines* **2015**, *3*, 27–54. [[CrossRef](#)]
2. Rahman, K.; Fahimi, B.; Suresh, G.; Rajarathnam, A.; Ehsani, M. Advantages of switched reluctance motor applications to EV and HEV: Design and control issues. *IEEE Trans. Ind. Appl.* **2000**, *36*, 111–121. [[CrossRef](#)]
3. Abdullah, H.; Ramasamy, G.; Ramar, K.; Aravind, C.V. Design consideration of dual axial flux motor for electric vehicle applications. In Proceedings of the 2015 IEEE Conference on Energy Conversion (CENCON), Johor Bahru, Malaysia, 19–20 October 2015; pp. 72–77.
4. Madhavan, R.; Fernandes, B.G. Axial Flux Segmented SRM with a Higher Number of Rotor Segments for Electric Vehicles. *IEEE Trans. Energy Convers.* **2013**, *28*, 203–213. [[CrossRef](#)]
5. Aydin, M.; Gulec, M.; Demir, Y.; Akyuz, B.; Yolacan, E. Design and validation of a 24-pole coreless axial flux permanent magnet motor for a solar powered vehicle. In Proceedings of the 2016 XXII International Conference on Electrical Machines (ICEM), Lausanne, Switzerland, 4–7 September 2016; pp. 1493–1498.
6. Yang, Y.-P.; Liang, J.-Y.; Xing, X.-Y. Design, and application of axial-flux permanent magnet wheel motors for an electric vehicle. In Proceedings of the AFRICON 2009, Nairobi, Kenya, 23–25 September 2009; pp. 1–5.
7. Gieras, J.F.; Wang, R.J.; Kamper, M.J. *Axial Flux Permanent Magnet Brushless Machines*; Springer Netherlands: Dordrecht, The Netherlands, 2008.
8. Hegazy, O.; Barrero, R.; Van Mierlo, J.; El Baghdad, M.; Lataire, P.; Coosemans, T. Control, analysis, and comparison of different control strategies of electric motor for battery electric vehicles applications. In Proceedings of the 2013 15th European Conference on Power Electronics and Applications (EPE), Lille, France, 2–6 September 2013; pp. 1–13.

9. Howlader, A.M.; Urasaki, N.; Senjyu, T.; Yona, A. Wide-Speed-Range optimal PAM control for permanent magnet synchronous motor. In Proceedings of the 2009 International Conference on Electrical Machines and Systems, Tokyo, Japan, 15–18 November 2009; pp. 1–5.
10. Shao, L.; Hua, W.; Zhu, Z.Q.; Tong, M.; Zhao, G.; Yin, F.; Wu, Z.; Cheng, M. Influence of Rotor-Pole Number on Electromagnetic Performance in 12-Phase Redundant Switched Flux Permanent Magnet Machines for Wind Power Generation. *IEEE Trans. Ind. Appl.* **2017**, *53*, 3305–3316. [[CrossRef](#)]
11. Zhu, J.; Cheng KW, E.; Xue, X. Torque analysis for in-wheel switched reluctance motors with varied number of rotor poles. In Proceedings of the 2016 International Symposium on Electrical Engineering (ISEE), Hong Kong, China, 14 December 2016; pp. 1–5.
12. Ji, J.; Luo, J.; Zhao, W. Relationship between iron loss and pole-pair number in flux-switching permanent-magnet machines. In Proceedings of the 2017 IEEE International Magnetics Conference (INTERMAG), Dublin, Ireland, 24–28 April 2017; pp. 1–6.
13. Magill, M.P.; Krein, P.T.; Haran, K.S. Equivalent circuit model for pole-phase modulation induction machines. In Proceedings of the 2015 IEEE International Electric Machines Drives Conference (IEMDC), Coeur d’Alene, ID, USA, 10–13 May 2015; pp. 293–299.
14. Reddy, B.P.; Umesh, B.S.; Rao, A.M.; Kumar, B.V.R.; Kumar, K.S. A five speed 45-phase induction motor drive with pole phase modulation for electric vehicles. In Proceedings of the 2017 IEEE International Conference on Industrial Technology (ICIT), Toronto, ON, Canada, 22–25 March 2017; pp. 258–263.
15. Takatsuka, Y.; Hara, H.; Yamada, K.; Maemura, A.; Kume, T. A wide speed range high efficiency EV drive system using winding changeover technique and SiC devices. In Proceedings of the 2014 International Power Electronics Conference (IPEC-Hiroshima 2014—ECCE ASIA), Hiroshima, Japan, 18–21 May 2014; pp. 1898–1903.
16. Swamy, M.M.; Kume, T.; Maemura, A.; Morimoto, S. Extended high-speed operation via electronic winding-change method for AC motors. *IEEE Trans. Ind. Appl.* **2006**, *42*, 742–752. [[CrossRef](#)]
17. Sergeant, P.; Vansompel, H.; Dupré, L.; Van den Bossche, A. Losses in VSI-PWM fed axial flux machines. In Proceedings of the 2014 16th European Conference on Power Electronics and Applications, Lappeenranta, Finland, 26–28 August 2014; pp. 1–6.